Neuron, Vol. 44, 1057–1066, December 16, 2004, Copyright ©2004 by Cell Press

# Frames of Reference for Eye-Head Gaze Commands in Primate Supplementary Eye Fields

**Julio C. Martinez-Trujillo,[1,2,*] W. Pieter Medendorp,[1,3] Hongying Wang,[1] and J. Douglas Crawford[1]**
[1]Laboratory of Visuomotor Neuroscience
Centre for Vision Research
Canadian Institutes of Health Research
Group for Action and Perception and
Departments of Psychology, Biology,
and Kinesiology and Health Sciences
CSB York University
Toronto, Ontario M3J 1P3
Canada
[2]Department of Physiology
Faculty of Medicine
McGill University
McIntyre Medical Sciences Building
3655 Promenade Sir William Osler
Montréal, Québec H3G 1Y6
Canada
[3]Nijmegen Institute for Cognition
and Information and
F.C. Donders Centre for Cognitive Neuroimaging
Radboud University Nijmegen
NL 6500 HE, Nijmegen
The Netherlands

## Summary

**The supplementary eye field (SEF) is a region within medial frontal cortex that integrates complex visuospatial information and controls eye-head gaze shifts. Here, we test if the SEF encodes desired gaze directions in a simple retinal (eye-centered) frame, such as the superior colliculus, or in some other, more complex frame. We electrically stimulated 55 SEF sites in two head-unrestrained monkeys to evoke 3D eye-head gaze shifts and then mathematically rotated these trajectories into various reference frames. Each stimulation site specified a specific spatial goal when plotted in its intrinsic frame. These intrinsic frames varied site by site, in a continuum from eye-, to head-, to space/body-centered coding schemes. This variety of coding schemes provides the SEF with a unique potential for implementing arbitrary reference frame transformations.**

## Introduction

Visual information enters the nervous system through photoreceptors that are fixed with respect to the eye, but this information must eventually be used to control muscles whose actions are fixed with respect to other body parts (e.g., head, torso, etc.). This necessitates an internal reference frame transformation (Soechting and Flanders, 1992; Andersen et al., 1993; Crawford and Guitton, 1997). Gaze control structures such as lateral intraparietal cortex (LIP) and the superior colliculus (SC) appear to encode gaze commands in a simple eye-centered reference frame (Cohen and Andersen, 2002; Colby et al., 1995; Klier et al., 2001). This has contributed to the conjecture that the early stages of visuomotor transformation rely almost exclusively on eye-centered coordinates, staving off the visuomotor reference frame transformation for later stages of processing (Klier et al., 2001; Andersen and Buneo, 2002).

In contrast, there is little consensus about the frames of reference for motor coding in the frontal cortex, particularly the supplementary eye field (SEF) (Schlag and Schlag-Rey, 1987; Russo and Bruce, 1996; Tehovnik et al., 1998). The SEF was originally defined as a dorsomedial area where low-intensity electrical stimulation evokes rapid eye movements (saccades), but it has since been implicated in the "higher" aspects of visuomotor transformation for saccades, such as target selection (Olson and Gettner, 1999; Stuphorn et al., 2000; Tremblay et al., 2002). Single-unit recordings have shown that SEF neurons can encode visual targets in both eye-centered and object-centered coordinates (Russo and Bruce, 1996; Olson and Gettner, 1999), but it is not known how the SEF transforms these signals into output commands. For example, its motor output command—as revealed in saccades evoked by electrical stimulation—has been variously suggested to code desired gaze targets in an eye-centered frame of reference (Russo and Bruce, 1996), a head-centered frame (Tehovnik et al., 1998), or multiple reference frames (Schlag and Schlag-Rey, 1987).

One explanation for this controversy is that previous stimulation studies were based on a two-dimensional (2D) analysis of small saccades evoked in head-restrained monkeys. We have recently shown that stimulation of the SEF in head-unrestrained animals results in larger gaze shifts composed of naturally coordinated eye and head movements (Martinez-Trujillo et al., 2003a). In such a system, gaze could be coded in any one of several frames of reference (Figures 1A–1C; see Results for further explanation). Some of these coding schemes—particularly the head-centered and space/body-centered schemes—are indistinguishable in the head-restrained animal.

Further, the eyes and head are capable of rotating with three degrees of freedom: vertical, horizontal, and torsional (about the line of site) (Glenn and Vilis, 1992). In the head-unrestrained animal, it is important to record all three dimensions, including torsion. This is not only because the eyes and head move torsionally during head-unrestrained gaze shifts (Klier et al., 2003), but also because three-dimensional (3D) representations are required to handle the nonlinear properties of rotation, which become prominent in large gaze shifts (Tweed and Vilis, 1987; Crawford et al., 2003). For example, the SC was once thought to code small gaze shifts using "fixed vector" commands (van Opstal et al., 1991) and larger gaze shifts using spatial goals (Straschill and Rieger, 1973), but it has recently been shown that this

*Correspondence: julio.martinez@mcgill.ca

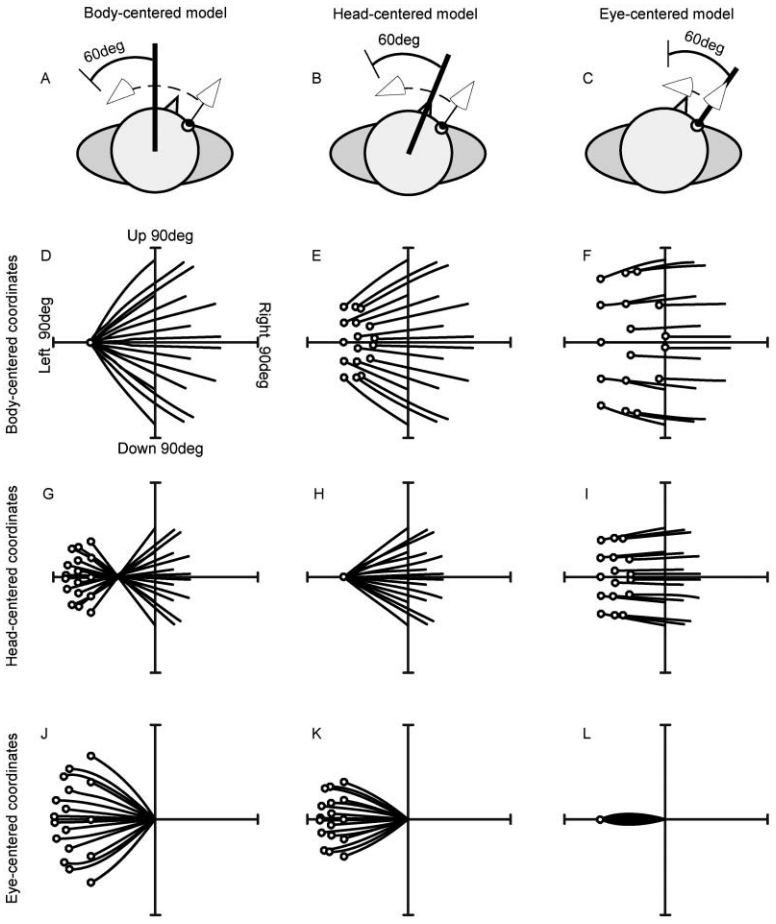


Figure 1. Model Simulations of Gaze Trajectories in Different Frames of Reference

A hypothetical subject fixates a target (white circle) with his body, head, and gaze pointing directions in misalignment. The subject has made a gaze shift toward a point located 60° to the left in space/body-centered coordinates (A), 60° to the left in head-centered coordinates (B), and 60° to the left in eye-centered coordinates (C). The dashed arrow indicates the gaze trajectory for each case, and the thick solid line indicates the sagittal axis orthogonal to the center of the reference frame. Simulated gaze trajectories from different initial gaze positions in space/body- (D), head- (E), and eye-centered (F) frames. The lines represent the trajectories, and the circles represent their final position; they are plotted in space/body-centered coordinates and as seen from behind. The abscissa represents the horizontal meridian, and the ordinate represents the vertical meridian. (G–I) Same data as in (D)–(F), but the trajectories are plotted in head-centered coordinates. (J–L) Same data as in (D)–(F) and (G)–(I), but the trajectories are plotted in eye-centered coordinates.

is simply the way an eye-centered representation of desired gaze projects onto 3D motor space (Klier et al., 2001).

Finally, it has been shown that in brain sites that code eye-head gaze shifts, the natural head contribution is required to reveal the actual goal of stimulus-evoked gaze shifts (Freedman et al., 1996; Roucoux et al., 1980; Martinez-Trujillo et al., 2003a, 2003b). For example, in our preliminary study of 23 SEF stimulation sites, "freeing" the head caused a general shift of the data from an apparent space/body-centered code toward an eye-centered coding scheme (Martinez-Trujillo et al., 2003b). But even so, the eye-centered model did not fit the SEF data as well as it fit the SC data (Klier et al., 2001), suggesting that a more complex analysis is required to understand the spatial coding of gaze commands in the SEF.

The purpose of the current study was to reexamine the question of gaze coding in the medial frontal cortex by (1) stimulating the macaque SEF while recording 3D eye and head rotations; (2) simulating the various possible motor frames that it might use to code gaze; and (3) using these simulations to inspire a mathematically correct 3D analysis of the data. Compared to our previous study (Martinez-Trujillo et al., 2003b), we obtained a much larger data set (i.e., more stimulation sites) and compared these to a more complete set of possible models, including one which has never been considered before (Figure 1B), using a more powerful set of analysis tools (multiple frames analysis). Based on the recent results of a similar study of the SC (Klier et al., 2001), and the observation that the SEF is functionally located upstream from the SC (Shook et al., 1990), we initially hypothesized that a simple eye-centered model would account for all of our SEF data, but as described in the Results, this assumption proved to be incorrect.

## Results

### Simulations of Gaze Coding in Different Reference Frames

What egocentric frames of reference might be used to code gaze in the SEF? Suppose that an SEF site drives gaze (using both the eyes and head) 60° left, as illustrated in Figure 1. The meaning of this statement depends on the frame of reference in which this command is defined. In our experiments, the torso was always restrained, so we will treat the space- and body-centered frames as equivalent (space/body). However, the eyes and head were free to move, so the space/body, head, and eye frames were ordinarily dissociated when the animals looked around. Therefore, depending on whether 60° left is defined in space/body-, head-, or eye-centered coordinates, this command would result in entirely different gaze shifts (as illustrated schematically in the top row of Figure 1).

In a space/body-centered frame (Figure 1A), the angle of the gaze shift required to drive gaze to the 60° left position is 100°, since initial gaze direction is oriented 40° to the right of the body's midline pointing direction. In a head-centered frame (Figure 1B), the required gaze shift is 80° degrees leftward, since initial gaze direction is oriented 20° to the right of the head's midline pointing direction. In an eye-centered frame (Figure 1C), the required gaze shift is 60° leftward, since the eye and gaze pointing directions are always aligned.

To illustrate the complete pattern in 2D, we simulated gaze trajectories (Figure 1, rows 2–4) from various natural combinations of initial 3D eye and head orientation (see Experimental Procedures), allowing the natural dissociation between the eye, head, and space/body frames. We set our model to provide a fixed 60° leftward output in space/body (left column), head (center column), or eye (right column) coordinates. We then plotted 2D gaze trajectories in space/body (row 2), head (row 3), or eye (row 4) coordinates. The resultant trajectory patterns are complex, reflecting the inherent nonlinearities of rotational geometry (Tweed and Vilis, 1987). However, one fundamental pattern emerges: each model produces gaze shifts that converge to a common location when plotted in its intrinsic coordinate system, i.e., the space/body model is plotted in space/body-centered coordinates (Figure 1D), the head model is plotted in head-centered coordinates (Figure 1H), and the eye model is plotted in eye-centered coordinates (Figure 1L). Plotted in other coordinates, the trajectories either diverge or fail to converge completely, depending on the model and coordinates of the plot.

The right column in Figure 1 (eye-centered model) simulates the results that were obtained in a previous experimental study of the SC (Klier et al., 2001). Would the same hold true for the SEF?

### Determining the Reference Frame for Gaze Coding in the SEF

If sites within the SEF encode a gaze motor output using one of the three frames simulated in Figure 1, then stimulation of these sites should reveal one of the three patterns (first, second, or third column) shown in this figure. We measured 3D eye and head rotations produced by delivering small electrical currents (of 50 μA and 300 Hz during 200 ms) into 55 different sites in the SEF of two macaques, designated as M1 and M2. These stimulation parameters have been shown to evoke kinematically normal gaze shifts when microstimulating the SEF (Martinez-Trujillo et al., 2003a) and the SC (Freedman et al., 1996; Klier et al., 2001) in macaques.

Figure 2 shows movement trajectories evoked by stimulating a site in the left SEF of animal M1 (Figure 2A). The lines represent the trajectories, and the open circles represent their landing positions. The stimulation-evoked gaze trajectories (Figure 2D) were composed of naturally combined movements of the eye in head (Figure 2B) and head in space (Figure 2C), illustrating our previous finding that the SEF encodes naturally coordinated eye-head gaze shifts (Martinez-Trujillo et al., 2003a). Moreover, gaze shifts (Figure 2D) started from a variety of different initial eye and head positions, as necessary for our reference frame analysis. Hence-

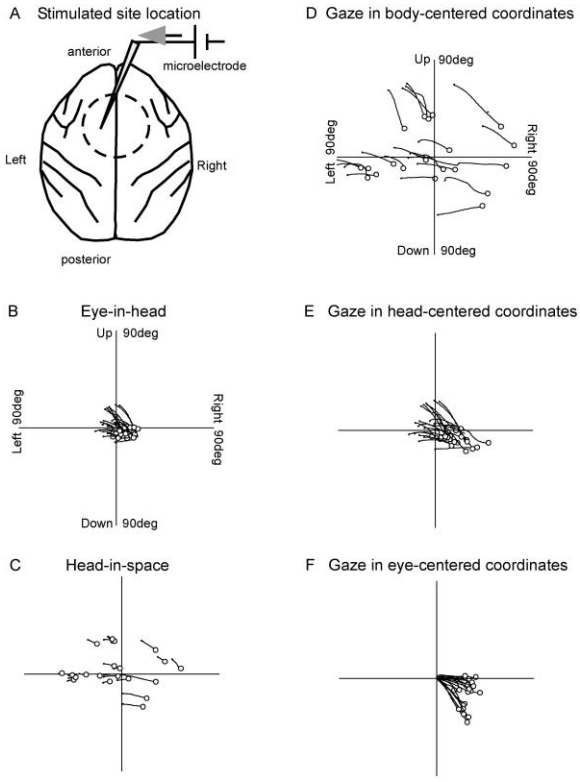


Figure 2. Example of Stimulation-Evoked Trajectories

(A) Top view of the brain hemispheres in animal M1; the tip of the electrode indicates the anatomical location of the stimulated site. The dashed circle indicates the recording chamber location.

(B) Behind view of the eye-in-head trajectories evoked by stimulating the site. The lines indicate the trajectories, and the small circles indicate their ending position. The abscissa represents the horizontal meridian, and the ordinate represents the vertical meridian.

(C) Behind view of the head-in-space trajectories. Symbols are the same as in (B).

(D–F) Gaze trajectories plotted in space/body- (D), head- (E), and eye-centered coordinates (F). Symbols are the same as in (B) and (C). The axes represent the horizontal (abscissa) and vertical (ordinate) meridians aligned with the center of the reference frame.

forth, we focus on the frame of reference for these gaze shifts.

The question is, do the gaze shifts evoked from this stimulation site converge toward some desired target direction? According to our simulations (Figure 1), they should when the data are plotted in the intrinsic coordinate system for that site. The right column in Figure 2 plots the stimulation-evoked gaze trajectories in three different coordinate systems in space/body-centered coordinates (Figure 2D), head-centered coordinates (Figure 2E), and eye-centered coordinates (Figure 2F). These plots follow the same format as the simulations in Figure 1. Although the general direction of the evoked gaze shifts (primarily down-right) is not the same as that in the simulations (leftward), this is not important; it is the general position-dependent pattern that matters.

A visual comparison between Figures 1 and 2 shows that this particular example does not follow the overall pattern predicted by the eye- or space/body-centered models, but rather follows the pattern of the head-cen-

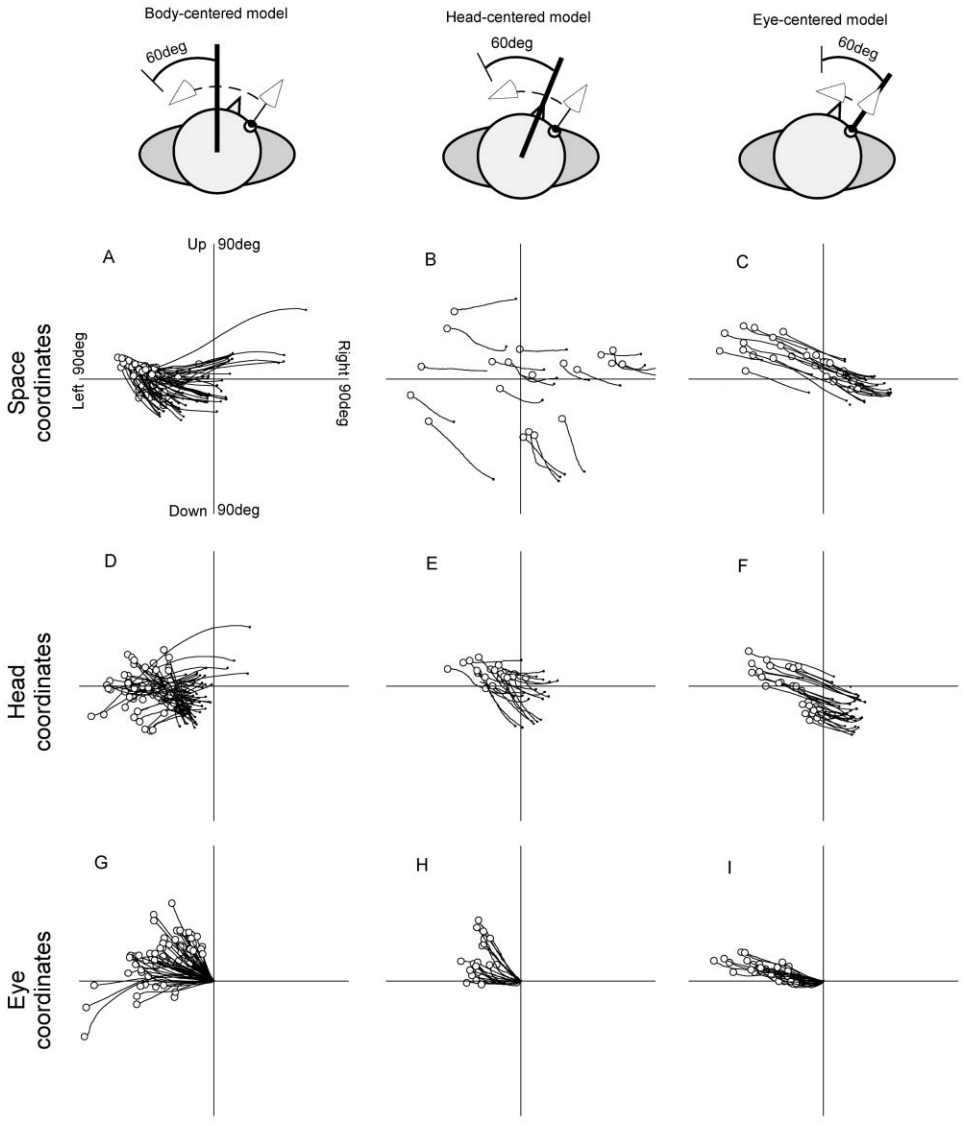


Figure 3. Stimulation Site Examples

Gaze trajectories from three different stimulated sites (columns) plotted in space/body (A, B, and C), head (D, E, and F), and eye (G, H, and I) coordinates. The symbols are the same as in Figure 2. The top row indicates the reference frame in which the trajectories are most likely encoded.

tered model (Figure 1, center column): insufficient convergence in space/body-centered coordinates, strong convergence in head-centered coordinates, and divergence in eye-centered coordinates. Remarkably, this particular SEF site appears to select a desired gaze direction that is fixed relative to the head (Figure 2E) and then drives both the eye (Figure 2B) *and* head (Figure 2C) in this direction until gaze is on target: a *head-centered* code for gaze. As we shall see, however, this was not the case for all sites.

We repeated the same visual analysis for all of our stimulation sites. Figure 3 shows gaze data from three example sites (arranged in the three columns). For easy comparison, we have plotted the data in the same format as Figure 1, i.e., in space/body-centered (second row), head-centered (third row), and eye-centered (fourth row). The cartoons in the first row illustrate the reference frame models that best fit the data in each column, when compared to the simulations (see plots along the main diagonal of the other three columns in Figure 1). We chose these three examples because they illustrate the main observations from our initial analysis. In a few sites, the highest convergence of the trajectories' final positions is in space/body coordinates (Figure 3, first column). In many sites, the data converged best in head-centered coordinates (Figure 3, second column). And for some sites, the evoked gaze shifts converged best when plotted in eye-centered coordinates (Figure 3, third column). Thus, these examples suggest that different SEF sites encode desired gaze direction in at least three different reference frames.

The simplest way to quantify these observations is to

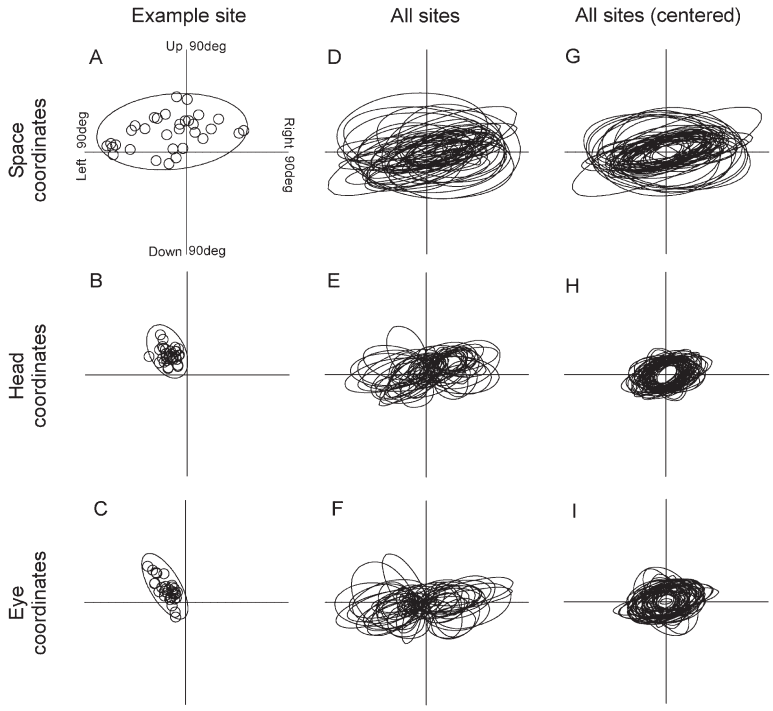


Figure 4. Gaze Convergence in Different Frames across Sites

(A–C) Trajectories' endpoints (open circles) and ellipse fitting in space/body (A), head (B), and eye (C) coordinates. The area of the ellipse indicates the convergence of the endpoints.

(D–F) Ellipses fitted to the endpoints of the stimulation-evoked gaze trajectories from the 49 sites in the two animals in space/body- (D), head- (E), and eye-centered (F) coordinates.

(G–I) Same data as in (D)–(F), but the ellipses have been translated in such a way that their centers coincide with the centers of the coordinate system.

focus on only the final gaze directions of the evoked movements, as an indicator of desired gaze direction for that site. In order to document this for all of our stimulation sites, we fit an ellipse to the cluster of gaze trajectory's endpoints in each coordinate system. This is a method of fitting and comparing the models: the coordinate system in which the ellipse is smallest corresponds to the coordinate frame model with the best fit.

Example ellipse fits are shown in the first column of Figure 4 for one site. The data points represent the endpoints of the trajectories plotted in space/body (first row), head (second row), and eye (third row) coordinates. The ellipse with the smallest area is the one corresponding to the head-centered plot, suggesting that this particular site encodes desired gaze relative to the pointing direction of the head. We repeated the same procedure for each of the stimulation sites and obtained the ellipses illustrated in the remainder of Figure 4. The second column shows the actual location of the gaze endpoint ellipses for the different sites, whereas the third column realigns them with the center of their coordinate systems for easier visual comparison of the ellipse areas.

Averaged across sites, the head-centered ellipse (Figure 4E) had the smallest area (1584$^{\circ 2}$), followed by the eye-centered ellipse (1753$^{\circ 2}$; Figure 4F) and space/body-centered ellipse (4383$^{\circ 2}$; Figure 4D). When comparing the areas of the ellipses among the three reference frames, we found that they were significantly smaller in head- and eye-centered coordinates than in space/body coordinates ($p < 0.0001$; Student's t test, after Bonferroni correction). However, we did not find statistically significant differences between the areas in head- and eye-centered coordinates ($p = 0.12$; paired Student's t test). On a site-by-site basis, the head frame model provided the best fit in 47% of the stimulation sites, with the eye frame and space/body frame providing a better fit in 38% and 15% of the sites, respectively.

Even when analyzed site by site, the ellipse fits were never perfect in any frame (this would have yielded a single point with zero area). This is not surprising considering the inherent state-dependent neural noise "downstream" of high-level structures like the SEF, which one would expect to randomly affect the results of individual stimulation trials. For example, when we filtered the same data using a conservative method that eliminates noise unrelated to any of the known reference frame models (but probably underestimates the noise relative to the real model for a given site), the average fit area dropped to 80% of its original value for the space/body model, 56% of its original value for the eye model, and 49% of its original value for the head model. Thus, part of the residual ellipse areas shown in Figures 4G–4I could be noise related. However, an inherent problem in this simple method of model fitting is that it assumes that each SEF sites perfectly follows one reference frame model, whereas in reality individual sites might fall within a continuum between these models.

To address these factors, we used a second, more complex method of quantification that did not rely solely on the potentially noisy endpoints of the gaze shifts and that allows one to visualize a complete continuum of representation. We quantified the convergence of the gaze trajectories as a function of initial gaze position and then plotted this as a function of the characteristic gaze displacement vector amplitude calculated for that site (see Experimental Procedures). We then compared these with the predictions of different models of gaze coding (Figure 5). A similar method was used in previous studies of the SC (Klier et al., 2001; Martinez-Trujillo et al., 2003b), but here, in order to test all possible models, we performed the analysis in multiple frames.

Figures 5A and 5B show a scatter plot analysis similar to that in our previous publications (Klier et al., 2001; Martinez-Trujillo et al., 2003b). Figure 5A shows conver-

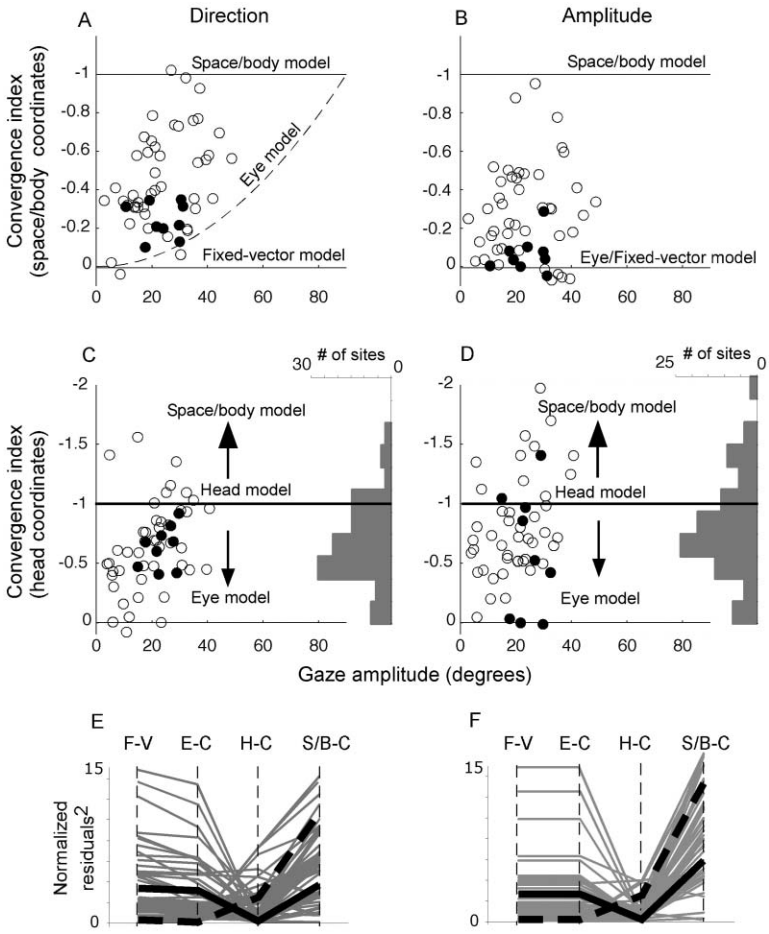


Figure 5. Convergence Indices in Different Frames

Convergence indices (ordinate) as a function of gaze amplitude (abscissa) for the direction (A and C) and amplitude (B and D) of the stimulation-evoked trajectories in space/body (A and B) and head (C and D) coordinates. Open circles correspond to data from animal M1, and filled circles correspond to data from M2. The right ordinate in (C) and (D) shows the distributions of the convergence indices. The graphs in the lower row show the residuals$^2$ for the fixed vector (F-V), eye-centered (E-C), head-centered (H-C), and space/body-centered (S/B-C) models for the convergence index for direction (E) and amplitude (F) of the movements. The thick solid black line shows an example site for which the head-centered model showed the lowest residuals, and the thick dashed black line shows an example for which the eye-centered model showed the lowest residuals.

gence indices (ordinate) for the component of gaze orthogonal to the characteristic gaze vector of each site (as a measure of directional convergence), and Figure 5B shows the convergence indices for the amplitude component of the gaze shifts (i.e., parallel to the characteristic gaze displacement vector), all plotted as a function of the characteristic gaze displacement amplitude for each site. The open circles represent data from one animal, and the filled circles represent the data from the second animal. Note that all of these data were computed in space/body-centered coordinates.

In these plots, a "fixed vector" model of gaze coding—independent of initial gaze position—predicts zero convergence (a horizontal line running along the abscissa), a space/body-centered coding predicts complete convergence in space (horizontal line at $-1$ in the ordinate), and an eye-centered model predicts a nonlinear curve (dashed line) in Figure 5A, with nearly zero convergence in Figure 5B (for a more complete description of the eye-centered model, see Klier et al., 2001).

Looking first at Figure 5A, unlike similarly plotted data from the SC (Klier et al., 2001), these data clearly do not follow the predictions of the eye-centered model (dashed line). The fit is even worse for the "fixed vector model." Nor do the data consistently follow the predictions of a space/body-centered model (horizontal line at $-1$ in the ordinate). Instead, they fall within the complete continuum between the eye-centered and space/body-centered models. This was also true for the convergence index (CI) for gaze amplitude (Figure 5B). Indeed, the convergence indices for these two components of gaze (plotted in Figures 5A and 5B) were correlated ($r > 0.6$ for the two animals).

One possibility is that the data fit best the predictions of a head-centered model. In the plots shown in Figures 5A and 5B, the predictions of a head-centered model cannot be represented by a single line, because they differ depending on the relative contributions of the eyes and head to gaze. This could be different for different animals, for different recording sites, and during different recording sessions. A large head contribution causes the head model to behave like the eye model, whereas a negligible head contribution causes the head model to become equal to the space/body model. Thus, in this plot one cannot distinguish whether the data are following the head model or falling within a true continuum, as suggested indirectly in our previous analysis (Figures 3 and 4). To address this issue, we performed a different analysis.

We first rotated the gaze trajectories for the different sites in head-centered coordinates and then recomputed the convergence indices for the direction and amplitude of the trajectories. This method allowed us to generate a single curve with the predictions of the head-centered model (horizontal line at $-1$ in the ordinate of the panels in the second row). In these plots

(Figures 5C and 5D), the data falling along the CI = −1 line fit better the predictions of the head-centered model, the data falling far below the line fit better the predictions of the eye-centered model, and the data falling well above the line fit better the predictions of the space/body-centered model. The frequency histograms on the left sides of these panels show that the full spectrum of models is represented in the SEF, but with the heaviest representation running from the eye-centered part of the range toward the head-centered part of the range.

To further quantify the above observations, we determined the goodness of fit of the data to the different models of gaze coding by computing the squared residuals between the data and the predictions of each model. In order to compare the residuals$^2$ in the head frame (Figures 5C and 5D) with those from the other plot (Figures 5A and 5B) on an even footing, we first normalized each residual$^2$ to the variance of the convergence indices of its correspondent distribution (see Experimental Procedures). The line graphs in Figures 5E and 5F show the distribution of the normalized residuals for the CI for the direction component (Figure 5E) and the amplitude component (Figure 5F) for the four models.

Considering the population as a whole, we found that for both convergence indices (direction and amplitude) the mean of the residuals$^2$ was significantly different across models ($p < 0.01$; Friedman test for repeated measurements) (Figure 5E and 5F). In the direction component, the head- and eye-centered models showed lower residual$^2$ values than the fixed vector and the space/body-centered model ($p < 0.01$; Dunn's multiple comparison test). In the amplitude component, the fixed vector, eye-centered, and head-centered models showed lower residuals than the space/body-centered model ($p < 0.01$ in all cases; Dunn's multiple comparison test). There was no significant difference between the eye- and head-centered models. However, the mean of the normalized residuals for the CI for direction was the lowest for the head-centered model (1.83 for the head-centered model, 3.07 for the eye-centered model, 3.69 for the fixed vector model, and 5.4 for the space/body-centered model).

When we examined the curves for individual sites (for example, the two highlighted curves for exemplary "eye" and "head" sites), we found that the head-centered model produced the lowest residuals in the most sites (26), followed by the eye-centered model (14 sites), the space/body model (eight sites), and finally the fixed vector model (only one site). This pattern of distribution agrees with the general pattern that was observed using the ellipse fit method (Figure 4). However, using the CI method (Figures 5A–5C) one can clearly see that the full distribution of data is best characterized as a continuum. In summary, our population of stimulation sites showed a continuum of coding between eye-centered to space/body-centered coding, with a propensity toward sites in the earlier eye- and head-centered coding range.

## Discussion

The current study recorded head-unrestrained gaze shifts evoked from a large set of electrically stimulated SEF sites, analyzed these data in 3D, and compared them to all known models of gaze coding in multiple reference frames. The results of this analysis were consistent with a continuum of coexisting eye-, head-, and space/body-centered representations for gaze coding in the SEF. This continuum could represent a gradual transformation from an eye-centered coding scheme to a space/body-centered coding scheme. However, it has been demonstrated in the past that such a transformation does not require explicit representations of the intermediate forms (Zipser and Andersen, 1988; Smith and Crawford, 2001). Therefore, we favor the alternative interpretation—that different sites within the SEF explicitly code gaze shifts in different reference frames in order to represent all possible contingencies for different task-related motor functions. Indeed, if our animals could move their bodies freely, one would also be able to test for truly space-centered (as opposed to body-centered) sites.

Previous studies have reported coding of saccadic eye movements in head-centered (Tehovnik et al., 1998), eye-centered (Russo and Bruce, 1996), and multiple reference frames (Schlag and Schlag-Rey, 1987) in the SEF. In light of our results, the apparent contradiction between these previous head-restrained studies is perhaps not surprising. First, because gaze coding in the SEF is so much more complex than gaze coding in, for example, the SC, and second, because with the head fixed the resulting gaze shift would be indeterminate, depending on the size of the movement, the animal's eye-head coordination strategy (Fuller, 1992), and training (Crawford and Guitton, 1997). As suggested previously, head-fixed stimulation is not an accurate measure of motor output in brain sites that code eye-head gaze (Martinez-Trujillo et al., 2003b; Freedman et al., 1996; Pare et al., 1994), and indeed freeing the body might further improve such data. In our study, however, we find elements of all those previous results in different aspects of our data, i.e., we find evidences in favor of the existence of multiple codes in the SEF, with a bias toward the head- and eye-centered coding schemes (Figure 5).

It is important to note that these coding schemes are not intrinsic to the SEF sites in isolation, but rather are the product of the total pattern of output connectivity activated when these sites were stimulated. Thus, the transformation from activity in the SEF to behavior depends on this full set of output targets and all of their downstream transformations, traced all the way to patterns of muscular activity. This would include projection to areas such as the frontal eye fields (Schall et al., 1993). It is possible that nonphysiological patterns of activation produced by our stimulation, such as activation of fibers en passant or nonphysiological combinations of SEF activity with other brain states, may have added noise to our results. However, our previous finding that SEF stimulation produces naturally coordinated eye-head gaze shifts (Martinez-Trujillo et al., 2003a) adds credence to our assumption that the coding schemes revealed in our experiment reveal aspects of normal physiology. Moreover, if gross electrical input to the SEF can evoke gaze shifts in multiple frames of references, it seems very likely that far more subtle phys-

iological patterns of input would be able to access *at least* these same patterns of motor output.

The second finding in our study was a predominance of head-centered representation of gaze in the SEF. This is a result that at first glance, due to its unfamiliarity, may sound contradictory. However, as illustrated in Figure 1B, this simply suggests that the motor output of the SEF codes a fixed goal with respect to the head—the effector(s) used is another matter. With a head-centered coding of gaze, desired gaze direction is defined with respect to initial head orientation (imagine a beam of light projected by a laser mounted on the head), but then both the eye and head are driven until gaze reaches that desired point. At the end of the gaze shift, the same site would then code a new direction in space, depending on final head orientation. As illustrated in our simulations (Figure 1, center column), a head-centered coding of gaze is quite feasible mathematically, and based on our stimulation data (e.g., Figure 2 and Figure 3, center column), some brain sites do appear to employ this coding scheme.

### Implications for the Gaze Control System

The results from the current study seem to be at odds with our current knowledge of gaze coding in the SC and posterior parietal cortex (PPC), both of which appear to employ an eye-centered code to control gaze (Colby et al., 1995; Klier et al., 2001; Cohen and Andersen, 2002). Not surprisingly, an eye-centered coding is still found in many of our SEF sites, but there were at least as many sites coding gaze in nonocular frames. It does not seem likely that the SEF is required to produce eye-to-head or eye-to-space reference frame transformations for all visuomotor transformations. In comparison, the eye-centered commands within the SC are much closer anatomically to the motoneurons (Klier et al., 2001), so it appears that the brainstem itself can transform eye-centered signals into muscle coordinates without the SEF. Thus, if the SEF is the odd one that does not speak the retinal (eye-centered) "lingua franca," there must be some special advantage to using a head- or space/body-centered output code for its particular function, compared to the simpler SC-brainstem visuomotor transformation.

One possibility is that these multiple coding schemes provide the basis for arbitrary "cognitive" coordinate transformations in the gaze control system. In other words, the SEF may combine visual information from multiple egocentric and object-centered frames (Olson and Gettner, 1999) into an abstract target salience map and transform these signals into gaze commands coded in any given frame required for a particular computation. This is consistent with the previous suggestion that premotor cortical structures such as the SEF are good candidates for performing nonstandard mappings between visual cues and motor commands, such as mapping arbitrary nonspatial cues (color) into specific motor commands for directing gaze in space (Wise et al., 1996). The capacity for arbitrary transformations would provide the SEF with the substrate for relatively complex "cognitive" computations beyond the capacity of the SC or FEF.

For example, the head-centered coding schemes observed in our data might not occur simply because the head code happens to fall at the center of the continuum from eye-centered to space/body-centered output coding, but rather because it fulfils some specific cognitive function. Consistent with the latter, a study (Scherberger et al., 2003) has recently reported behavioral evidence that target selection in macaque monkeys—thought to be one important function of the frontal cortex (Schall, 1991a, 1991b; Coe et al., 2002)—is mediated in head-centered coordinates. This being the case, then further transformations would be required to communicate such codes with the simpler eye-centered gaze control structures. In support of this idea, projections from the SEF to the FEF diverge significantly, providing a possible structural pathway for an intermediate reference frame transformation (Schall et al., 1993; Stanton et al., 1993).

Based on these factors and other findings (Olson and Gettner, 1999; Schiller et al., 1987), we suggest two separate streams in the visuomotor transformations for gaze control—one for direct, visually guided action, going through the parietal lobe and then through the SC, where the visuomotor reference frame transformation would only occur in the brainstem. The second stream performs more complex visuospatial and cognitive tasks (involving top-down attention and target selection in arbitrary visual reference frames) and proceeds from the parietal lobe through the SEF, and from there to the FEF and other cognitive and motor systems. The FEF might play an important role in the second stream by conveying information from the SEF to the SC (Huerta et al., 1986; Everling and Munoz, 2000). An important question to answer in further studies is how the use of these different streams and reference frames is influenced by specific task demands.

## Experimental Procedures

### Computer Simulations

Simulated gaze trajectories were generated with the use of a previously published 3D eye-head coordination model (Tweed, 1997). This model was originally designed to use as input an internal estimate of desired gaze direction relative to the eye. This variable, expressed as a unit vector ($G_{eye}$), is continuously updated in the model by using internal feedback signals coding eye and head motion. Simulations of the eye-centered model for various initial eye and head positions are shown in Figure 1 (right column). In order to generate predictions for gaze shifts encoded in a head-centered or space/body-centered frame, we assumed a fixed input vector at these levels ($G_{head}$ and $G_{space}$, respectively). This vector was then recomputed in the appropriate (retinal) coordinates for the model to be able to generate its predictions (using the formulas $G_{eye} = q_{Ei}^{-1} \times G_{head} \times q_{Ei}$ and $G_{eye} = q_{Es}^{-1} \times G_{head} \times q_{Es}$, respectively, where $q_{Ei}$ is the initial eye-in-head quaternion and $q_{Es}$ is the initial eye-in-space quaternion). The initial eye and head positions used in the simulations were used to compute the simulated gaze directions in either space/body-, head-, or eye-centered coordinates.

### Experiments

Two *Maccaca mulatta* were prepared for 3D eye and head movement recordings. Each animal underwent a surgical procedure under general anesthesia, during which we implanted 3D custom-made coils (copper wired) on the right eye and a stainless steel head post and a recording chamber (Crist Instruments) on the skull embedded on an acrylic cap. The recording chamber (20 mm diameter) was positioned at 25 mm anterior and 0 mm lateral in stereotaxic coordinates, giving access to both SEFs through a craniotomy of the frontal bone. All these procedures were in accordance with the

Canadian Council on Animal Care guidelines and were preapproved by the York University Animal Care Committee.

During the experiments, the animals wore primate jackets that constrained the movements of the torso but allowed them to freely move their heads (for more details, see Martinez-Trujillo et al., 2003a). Animals were trained (head unrestrained) to direct their gaze toward the location of an LED previously flashed during 500 ms. If gaze was maintained at that location during a 2000 ms period and within a 5°–20° diameter fixation window, a drop of juice was given to the animal. In trials where microstimulation was not used, the animals performed correctly in more than 80% of the cases.

One to three electrode penetrations were made during each experimental session using a microdrive (Narishigi model MO-99S) positioned on the top of a recording chamber and Platinum-Iridium glass-covered microelectrodes (FHC Inc.; impedance 0.5–3 MΩ). The electrode was advanced until single or multiunit activity was visualized on an oscilloscope, and then microstimulation trains were delivered (10 to 20 trains with intensities of 50 μA, durations of 200 ms, and frequencies of 300 Hz) at a random time within the 2000 ms fixation period following the LED flash, when no visual stimulus was present (Tehovnik et al., 1999).

A total of 82 SEF sites were identified. Of these, eye and head movements were evoked with consistent latencies in 55 (45 in M1 and 10 in M2). We only quantitatively analyzed data from sites in which we evoked at least 20 movements from different initial gaze positions, distributed approximately equally around the center. A total of 49 sites (39 in M1 and 9 in M2) met this condition. We did not systematically stimulate using other parameters, because our previous study suggested that these parameters evoked naturally coordinated eye-head gaze shifts (Martinez-Trujillo et al., 2003a).

### Data Analysis

From the raw coil signals, we computed quaternions (q) representing the orientation of the eye in space (Es) and head in space (Hs) with respect to a reference position in which the eyes and the head were pointing straight ahead. This kind of representation when expressed in a right hand rule coordinate system aligned with the coils has proven to be accurate for measuring 3D eye and head rotations during gaze movements (Tweed et al., 1990). From the eye-in-space (Es) and head-in-space (Hs) quaternions, we computed the eye-in-head (Eh) quaternions (Crawford and Guitton, 1997) by using the formula $qEh = qHs \times qEs^{-1}$.

Quaternions representing the Es trajectories were transformed into eye-centered coordinates (Figure 4, last column from left to right) by using first the formula $q_{Ec} = q_{Es} \times q_{Esi}^{-1}$ that multiplies the Es quaternions ($q_{Es}$) by the inverse of the Es quaternion representing the eye-in-space position at the beginning of the movement ($q_{Esi}^{-1}$). $q_{Ec}$ represents the quaternions in eye-centered coordinates. In a similar manner, we transformed the Es quaternions into head-centered coordinates ($q_{Hc}$) by using the formula $q_{Hc} = q_{Es} \times q_{Hsi}^{-1}$, which multiplies the Es quaternions ($q_{Es}$) by the inverse of the head-in-space quaternion at the beginning of the movements ($q_{Hsi}^{-1}$). The space/body-centered coordinates' quaternions were simply the Es quaternions, since during our experiments the bodies of the animals were restrained. The quaternions in the different coordinate systems were converted into 3D vectors scaled by their angle of rotation (Crawford and Guitton, 1997).

In order to determine the goodness of fit of our data to each model, we computed the convergence of the movements in each coordinate system by fitting an ellipse to the endpoints of the gaze trajectories using the least-squares method. From the parameters of the ellipse, we computed its area using the formula area $= \Pi \times A \times B$, where A and B are the major and minor radius of the ellipse. This area is an estimate of gaze convergence in the different frames. The comparisons among the areas of the ellipses were conducted using a paired Student's t test.

For the data analysis shown in Figure 5, we first computed the characteristic vector (CV) for each site through a multiple linear regression procedure relating the stimulation-evoked displacement of gaze trajectories as a function of initial gaze position. The CV of a given site represents the theoretical gaze trajectory that would be evoked by stimulating the site when the animal is looking straight ahead. Once the CV was obtained, we aligned all the trajectories and the characteristic vector with the horizontal meridian. For each individual trajectory, we measured its initial position (IP) and final position (FP) along the abscissa and the ordinate, and by subtracting them we obtained the gaze displacement along both axes (FPx − IPx; Fpy − IPy). A convergence index for the movements' direction (CId) was computed by determining the slope of the regression line relating the initial position (IPy) and the gaze displacement (FPy − IPy) along the ordinate. A convergence index for the movements' amplitude (CIa) was computed by determining the slope of the regression line relating the initial position (IPx) and the gaze displacement (FPx − IPx) along the abscissa (Martinez-Trujillo et al., 2003b; Klier et al., 2001; Russo and Bruce, 1996).

For the plots shown in Figures 5A and 5B, the convergence indices and CV were computed in space/body-centered coordinates. For the convergence indices and CV shown in Figures 5C and 5D, the data were first transformed into head-centered coordinates. The normalized residuals appearing in Figures 5E and 5F were computed by first calculating the residuals squared between the CIs of the stimulation-evoked data appearing in Figures 5A–5D and the CIs predicted by the different models (CIp) for each site $(CI - CIp)^2$. Second, we normalized these squared residuals to the variance (Vr) of the correspondent convergence index distribution (i.e., $[CI - CIp]^2/Vr$). This latter normalization was conducted in order to make comparable the data plotted in the different reference frames (i.e., space-centered [Figures 5A and 5A] and head-centered [Figures 5C and 5D]), which had different variances.

For the noise analysis on our ellipse data, predicted gaze trajectories were obtained by fitting the following model to the stimulation data: $Gf(h, v) = a1 + a2 \times Gi(h) + a3 \times Gi(v) + a4 \times Gi(t) + a8 \times Hi(h) + a9 \times Hi(v) + a10 \times Hi(t)$, where Gf and Gi represent final and initial gaze positions, respectively; Hi represents initial head position; and h, v, and t represent the horizontal, vertical, and torsional components of gaze and head. The model's coefficients are represented by a(i). After obtaining the coefficients, we computed the predicted final gaze positions in space/body-, head-, and eye-centered coordinates from the initial gaze and head positions. This represents only the components of the trajectories that could be predicted based on some reference frame model.

### Anatomical Reconstruction of the Recording Sites

After the experiments, the two animals were sacrificed, and anatomical reconstructions of the stimulation sites were made. Our reconstruction of the stimulation sites in the two animals that participated in the current experiments can be found elsewhere (Martinez-Trujillo et al., 2003a). We also tested whether the stimulation sites followed any topographical pattern by mapping the quantitative parameters related to our spatial coding schemes (Figure 5) in stereotaxic coordinates. However, we found no consistent pattern of results in our data sample.

### Acknowledgments

The authors thank Saihong Sun, Tyrone Lew, Lydia Troc, and Natasha Down for technical assistance. This work was supported by a Canadian Institutes of Health Research (CIHR) grant and Premier's Research Excellence Award to J.D.C. During this study, J.C.M.-T. was supported by the CIHR Strategic Training Program in Vision Health Research; W.P.M. was supported by a Human Frontiers Long-Term Fellowship; and J.D.C. was supported by a Canada Research Chair.

Received: May 27, 2004
Revised: September 7, 2004
Accepted: November 10, 2004
Published: December 15, 2004

### References

Andersen, R.A., and Buneo, C.A. (2002). Intentional maps in posterior parietal cortex. Annu. Rev. Neurosci. *25*, 189–220.

Andersen, R.A., Snyder, L.H., Li, C.S., and Stricanne, B. (1993). Coordinate transformations in the representation of spatial information. Curr. Opin. Neurobiol. *3*, 171–176.

Coe, B., Tomihara, K., Matsuzawa, M., and Hikosaka, O. (2002). Visual and anticipatory bias in three cortical eye fields of the monkey during an adaptive decision-making task. J. Neurosci. *22*, 5081–5090.

Cohen, Y.E., and Andersen, R.A. (2002). A common reference frame for movement plans in the posterior parietal cortex. Nat. Rev. Neurosci. *3*, 553–562.

Colby, C.L., Duhamel, J.R., and Goldberg, M.E. (1995). Oculocentric spatial representation in parietal cortex. Cereb. Cortex *5*, 470–481.

Crawford, J.D., and Guitton, D. (1997). Primate head-free saccade generator implements a desired (post-VOR) eye position command by anticipating intended head motion. J. Neurophysiol. *78*, 2811–2816.

Crawford, J.D., Martinez-Trujillo, J.C., and Klier, E.M. (2003). Neural control of three-dimensional eye and head movements. Curr. Opin. Neurobiol. *13*, 655–662.

Everling, S., and Munoz, D.P. (2000). Neuronal correlates for preparatory set associated with pro-saccades and anti-saccades in the primate frontal eye field. J. Neurosci. *20*, 387–400.

Freedman, E.G., Stanford, T.R., and Sparks, D.L. (1996). Combined eye-head gaze shifts produced by electrical stimulation of the superior colliculus in rhesus monkeys. J. Neurophysiol. *76*, 927–952.

Fuller, J.H. (1992). Head movement propensity. Exp. Brain Res. *92*, 152–164.

Glenn, B., and Vilis, T. (1992). Violations of Listing's law after large eye and head gaze shifts. J. Neurophysiol. *68*, 309–318.

Huerta, M.F., Krubitzer, L.A., and Kaas, J.H. (1986). Frontal eye field as defined by intracortical microstimulation in squirrel monkeys, owl monkeys, and macaque monkeys: I. Subcortical connections. J. Comp. Neurol. *253*, 415–439.

Klier, E.M., Wang, H., and Crawford, J.D. (2001). The superior colliculus encodes gaze commands in retinal coordinates. Nat. Neurosci. *4*, 627–632.

Klier, E.M., Martinez-Trujillo, J.C., Medendorp, W.P., Smith, M.A., and Crawford, J.D. (2003). Neural control of 3-D gaze shifts in the primate. Prog. Brain Res. *142*, 109–124.

Martinez-Trujillo, J.C., Wang, H., and Crawford, J.D. (2003a). Electrical stimulation of the supplementary eye fields in the head-free macaque evokes kinematically normal gaze shifts. J. Neurophysiol. *89*, 2961–2974.

Martinez-Trujillo, J.C., Klier, E.M., Wang, H., and Crawford, J.D. (2003b). Contribution of head movement to gaze command coding in monkey frontal cortex and superior colliculus. J. Neurophysiol. *90*, 2770–2776.

Olson, C.R., and Gettner, S.N. (1999). Macaque SEF neurons encode object-centered directions of eye movements regardless of the visual attributes of instructional cues. J. Neurophysiol. *81*, 2340–2346.

Pare, M., Crommelinck, M., and Guitton, D. (1994). Gaze shifts evoked by stimulation of the superior colliculus in the head-free cat conform to the motor map but also depend on stimulus strength and fixation activity. Exp. Brain Res. *101*, 123–139.

Roucoux, A., Guitton, D., and Crommelinck, M. (1980). Stimulation of the superior colliculus in the alert cat. II. Eye and head movements evoked when the head is unrestrained. Exp. Brain Res. *39*, 75–85.

Russo, G.S., and Bruce, C.J. (1996). Neurons in the supplementary eye field of rhesus monkeys code visual targets and saccadic eye movements in an oculocentric coordinate system. J. Neurophysiol. *76*, 825–848.

Schall, J.D. (1991a). Neuronal activity related to visually guided saccadic eye movements in the supplementary motor area of rhesus monkeys. J. Neurophysiol. *66*, 530–558.

Schall, J.D. (1991b). Neuronal activity related to visually guided saccades in the frontal eye fields of rhesus monkeys: comparison with supplementary eye fields. J. Neurophysiol. *66*, 559–579.

Schall, J.D., Morel, A., and Kaas, J.H. (1993). Topography of supplementary eye field afferents to frontal eye field in macaque: implications for mapping between saccade coordinate systems. Vis. Neurosci. *10*, 385–393.

Scherberger, H., Goodale, M.A., and Andersen, R.A. (2003). Target selection for reaching and saccades share a similar behavioral reference frame in the macaque. J. Neurophysiol. *89*, 1456–1466.

Schiller, P.H., Sandell, J.H., and Maunsell, J.H. (1987). The effect of frontal eye field and superior colliculus lesions on saccadic latencies in the rhesus monkey. J. Neurophysiol. *57*, 1033–1049.

Schlag, J., and Schlag-Rey, M. (1987). Evidence for a supplementary eye field. J. Neurophysiol. *57*, 179–200.

Shook, B.L., Schlag-Rey, M., and Schlag, J. (1990). Primate supplementary eye field: I. Comparative aspects of mesencephalic and pontine connections. J. Comp. Neurol. *301*, 618–642.

Smith, M.A., and Crawford, J.D. (2001). Self-organizing task modules and explicit coordinate systems in a neural network model for 3-D saccades. J. Comput. Neurosci. *10*, 127–150.

Soechting, J.F., and Flanders, M. (1992). Moving in three-dimensional space: frames of reference, vectors, and coordinate systems. Annu. Rev. Neurosci. *15*, 167–191.

Stanton, G.B., Bruce, C.J., and Goldberg, M.E. (1993). Topography of projections to the frontal lobe from the macaque frontal eye fields. J. Comp. Neurol. *330*, 286–301.

Straschill, M., and Rieger, P. (1973). Eye movements evoked by focal stimulation of the cat's superior colliculus. Brain Res. *59*, 211–227.

Stuphorn, V., Taylor, T.L., and Schall, J.D. (2000). Performance monitoring by the supplementary eye field. Nature *408*, 857–860.

Tehovnik, E.J., Slocum, W.M., Tolias, A.S., and Schiller, P.H. (1998). Saccades induced electrically from the dorsomedial frontal cortex: evidence for a head-centered representation. Brain Res. *795*, 287–291.

Tehovnik, E.J., Slocum, W.M., and Schiller, P.H. (1999). Behavioural conditions affecting saccadic eye movements elicited electrically from the frontal lobes of primates. Eur. J. Neurosci. *11*, 2431–2443.

Tremblay, L., Gettner, S.N., and Olson, C.R. (2002). Neurons with object-centered spatial selectivity in macaque SEF: do they represent locations or rules? J. Neurophysiol. *87*, 333–350.

Tweed, D. (1997). Three-dimensional model of the human eye-head saccadic system. J. Neurophysiol. *77*, 654–666.

Tweed, D., and Vilis, T. (1987). Implications of rotational kinematics for the oculomotor system in three dimensions. J. Neurophysiol. *58*, 832–849.

Tweed, D., Cadera, W., and Vilis, T. (1990). Computing three-dimensional eye position quaternions and eye velocity from search coil signals. Vision Res. *30*, 97–110.

Van Opstal, A.J., Hepp, K., Hess, B.J., Straumann, D., and Henn, V. (1991). Two- rather than three-dimensional representation of saccades in monkey superior colliculus. Science *252*, 1313–1315.

Wise, S.P., di Pellegrino, G., and Boussaoud, D. (1996). The premotor cortex and nonstandard sensorimotor mapping. Can. J. Physiol. Pharmacol. *74*, 469–482.

Zipser, D., and Andersen, R.A. (1988). A back-propagation programmed network that simulates response properties of a subset of posterior parietal neurons. Nature *331*, 679–684.